FRIEDRICH-SCHILLER-
UNIVERSITÄT
JENA

Quantum Memories & Repeaters

~ The art of delaying decoherence long enough to brag about it

Vishnuthirtha Sandur Huliraj
MSc Quantum Science and Technology
FSU Jena

Contents

Why Quantum Repeaters?

- Fiber loss scales exponentially
- At 1000 km, efficiency hits 10^{-20} taking centuries to transmit a single photon.

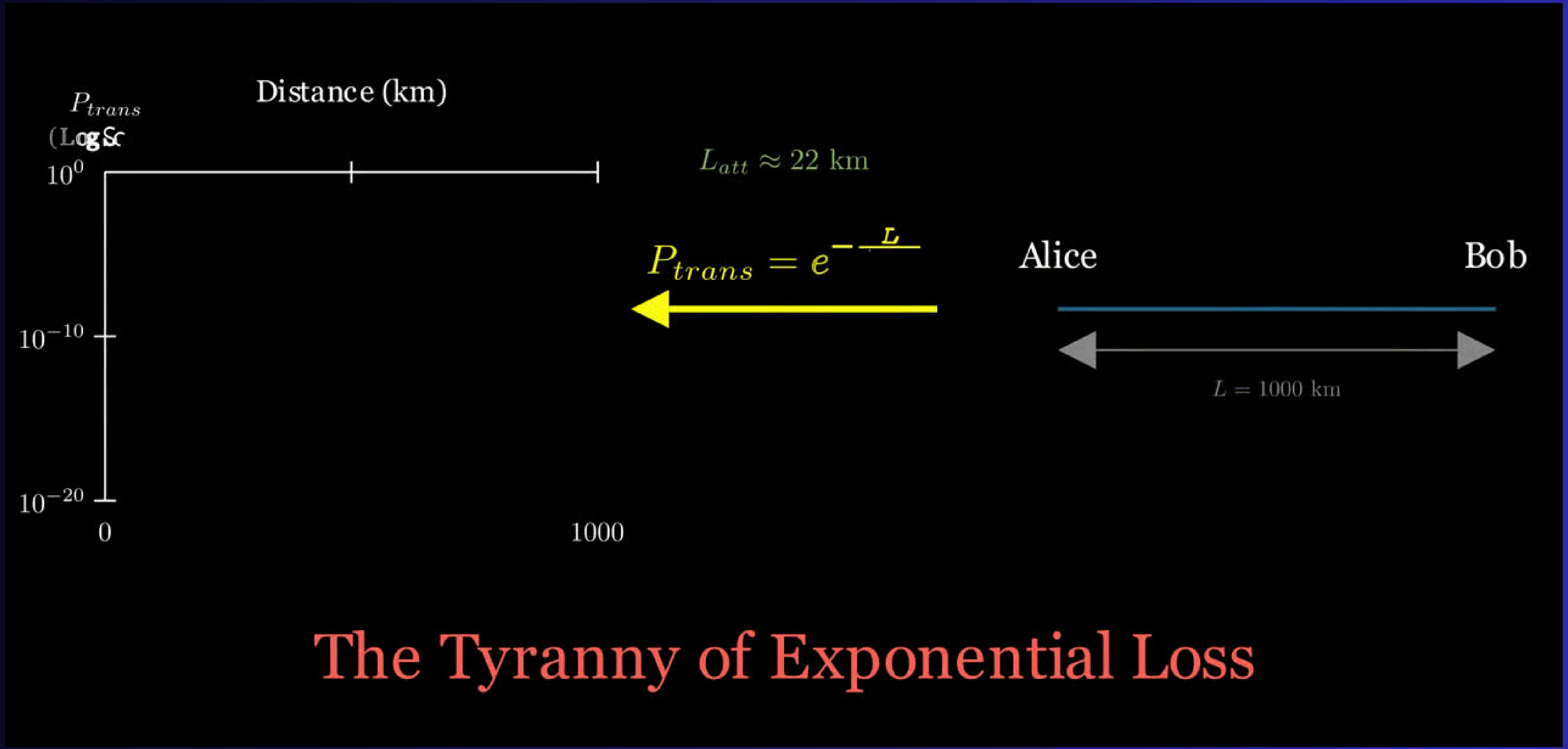

Fig 1: Visualization for Direct Quantum Communication (without Quantum Repeater) [16]

Why Quantum Repeaters?

- The repeater breaks the total distance into smaller segments (e.g., 2 segments of length L/2)
- The probability now scales with the segment length, not the total length.

$$P_{direct} \propto e^{-\frac{L}{L_{att}}} \xrightarrow{\text{segments } L \to L/2} P_{repeater} \propto e^{-\frac{L}{2L_{att}}} \tag{1}$$

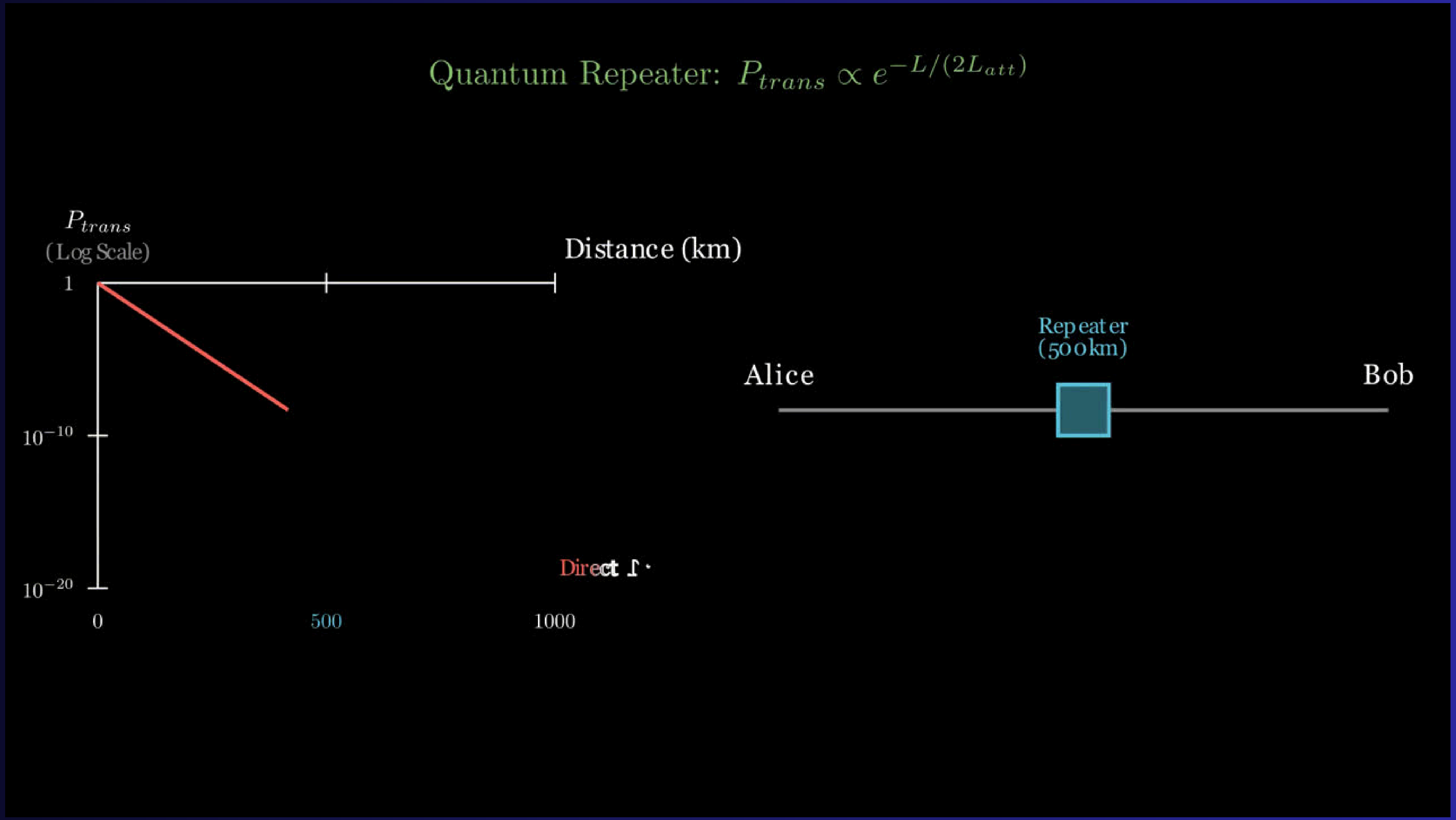

Fig 2: Visualization for Quantum Communication with Quantum Repeater [16]

Quantum Repeaters

Quantum Repeaters

A Quantum Repeater is not an amplifier (which copies signals). It is a device that distributes entanglement over long distances by breaking the channel into smaller, manageable segments.

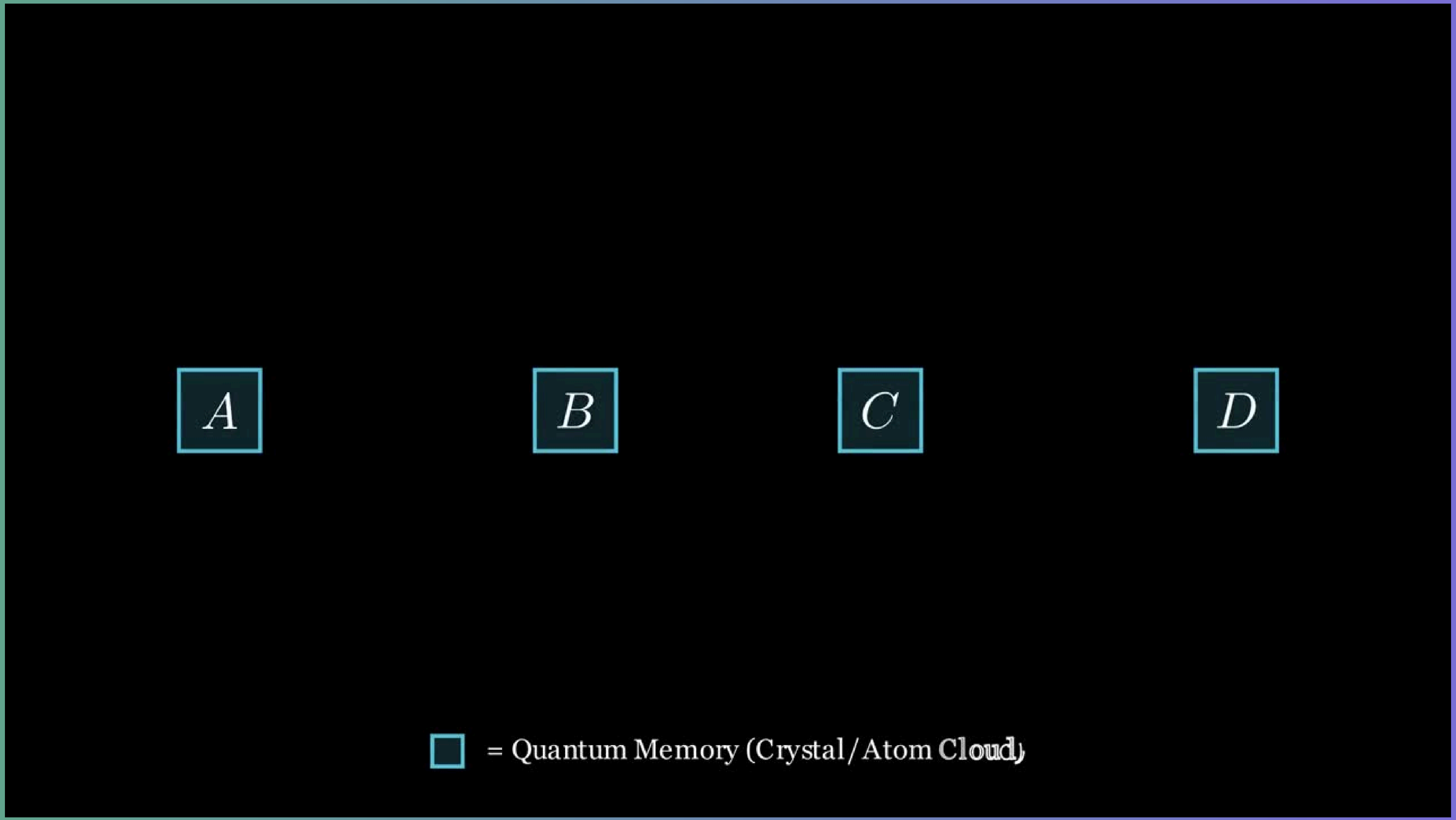

Fig 3: Visualisation of Quantum Repeater

Quantum Repeaters

Initialization (Entangle & Store)

- We have the system as follows,

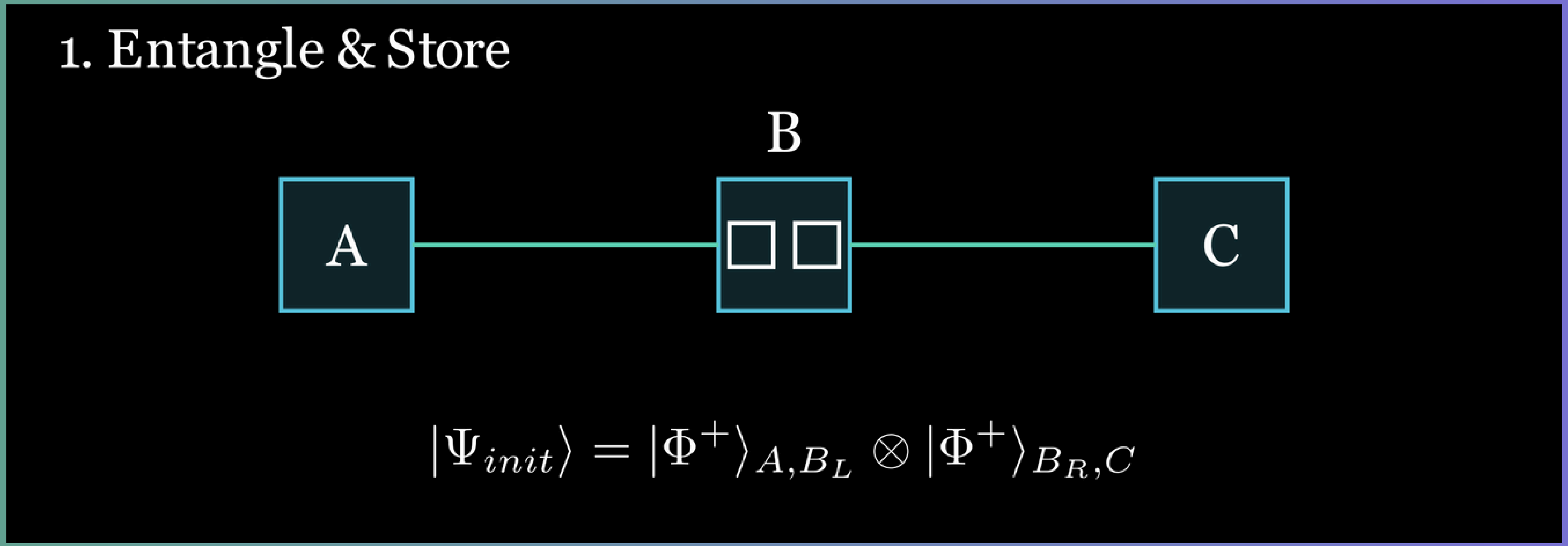

Fig 4: Illustration of Initialization step

Intermediate nodes (B & C) must hold two distinct qubits in memory: a "Left" qubit (L) and a "Right" qubit (R).

- Each link is initialized in a maximally entangled Bell State (Φ^+)
- Since the two links are created simultaneously and independently, the total Hilbert space is the Tensor Product of the individual pairs

Quantum Repeaters

Bell State Measurement (Entanglement Swapping)

- Node B performs a joint Bell State Measurement (BSM) on its two stored qubits.
- Rewriting the state of the 4 qubits in the Bell basis

$$\underbrace{|\Phi^+\rangle_{A,B_L} \otimes |\Phi^+\rangle_{B_R,C}}_{\text{Two Independent Pairs}} = \frac{1}{2}\sum_{k=1}^{4} \underbrace{|\sigma_k\rangle_{A,C}}_{\text{New Link}} \otimes \underbrace{|\beta_k\rangle_{B_L,B_R}}_{\text{Measurement at B}} \quad (2)$$

- Measurement at Node B, finds a specific result, which mathematically shows the global wavefunction
- Nodes A and C are now in entangled Bell State $|\Phi^+\rangle_{AC}$

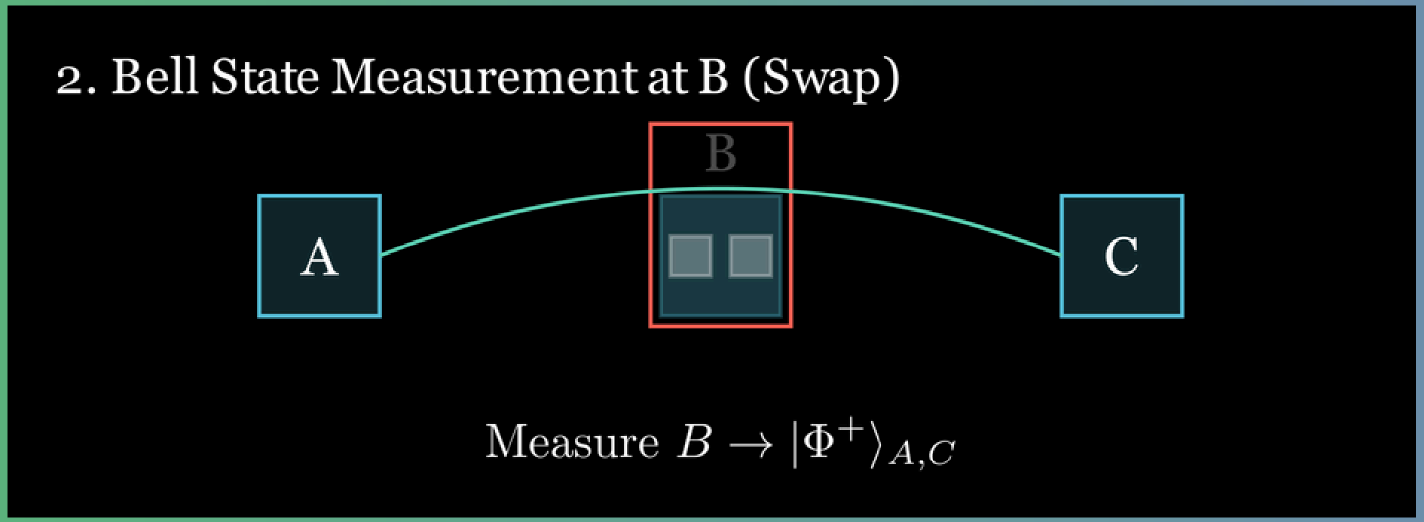

Fig 5: Illustration of BSM

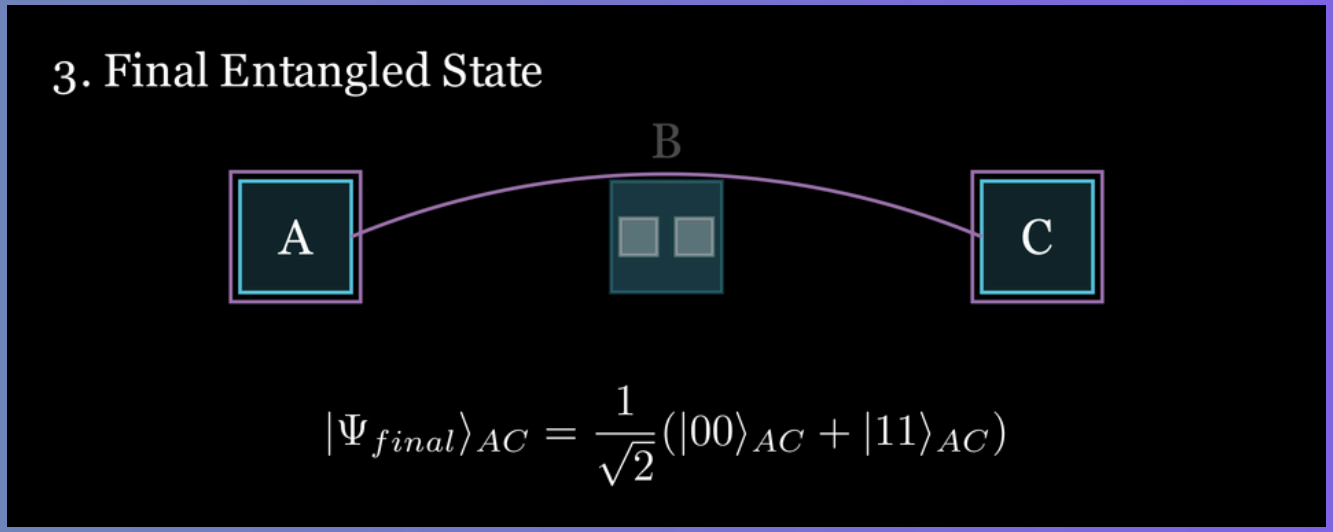

Fig 6: Illustration of Final Step

We have successfully 'teleported' the entanglement across the chain. A and D can now use this link for Quantum Key Distribution (QKD) or teleportation, exactly as if they were right next to each other.

Core Component of Quantum Repeaters

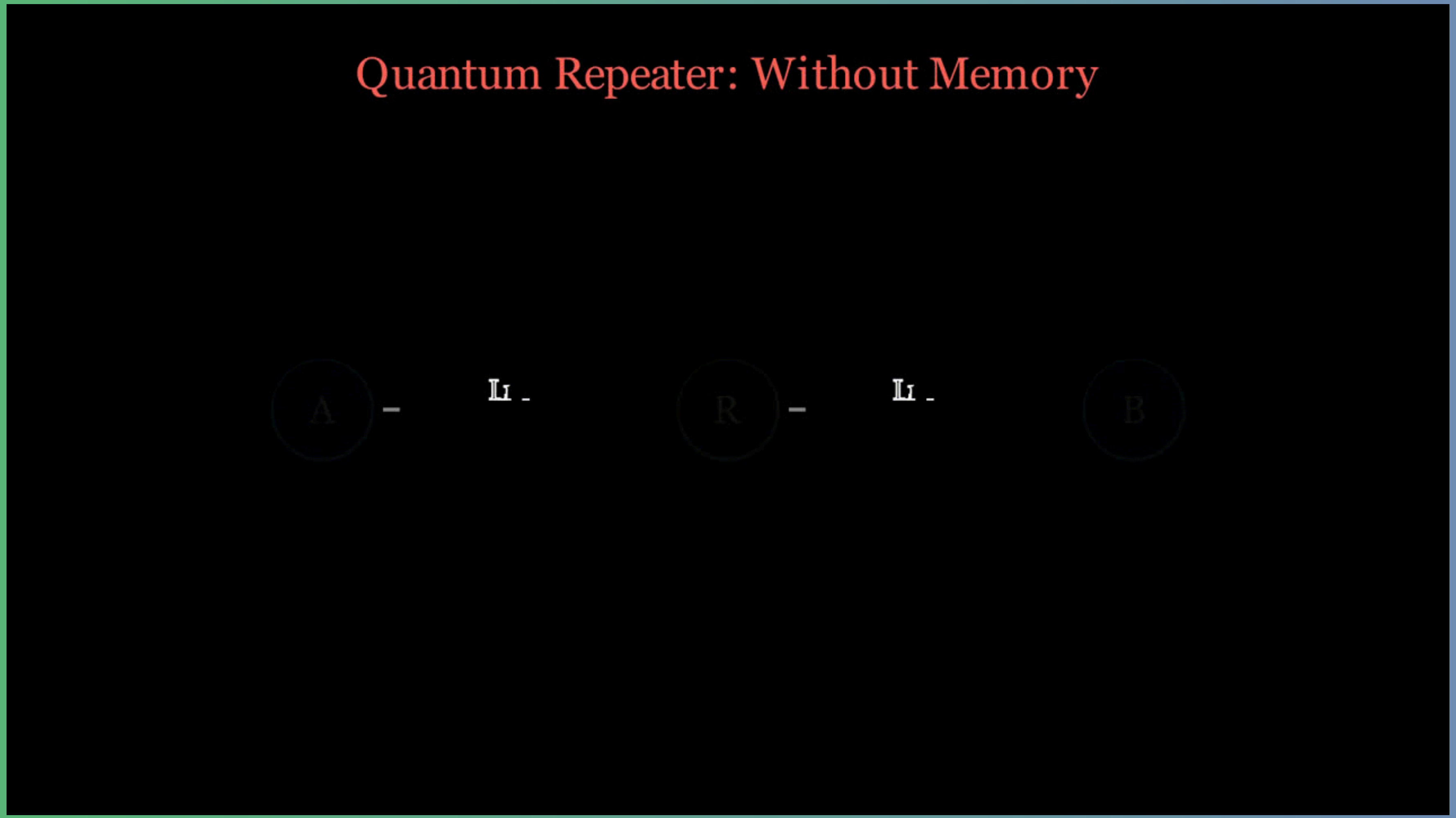

Fig 7: Illustration of case without Quantum Memory

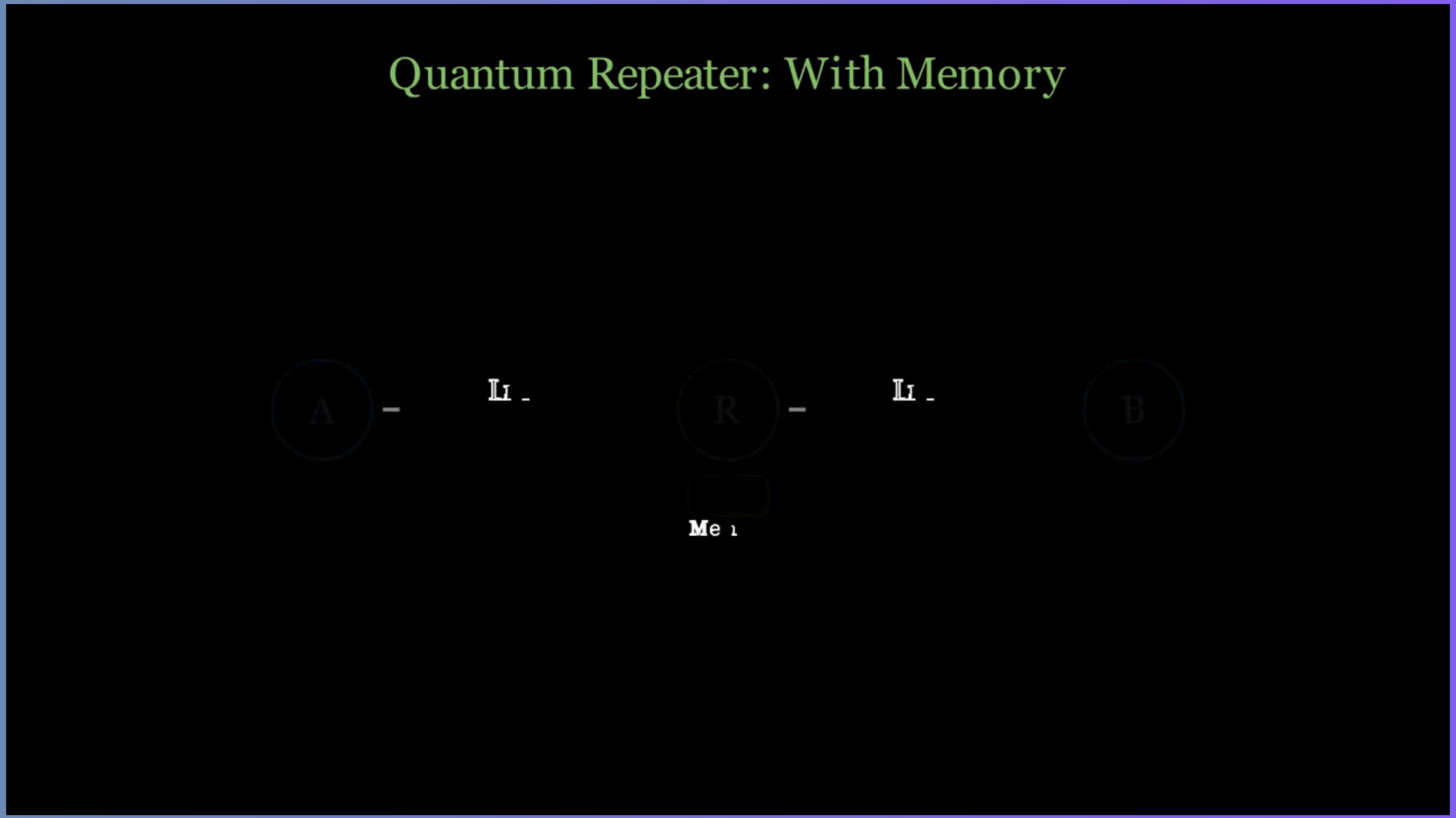

Fig 8: Illustration of case with Quantum Memory

$$P_{success} = p1 \times p2 = 0.25 \times 0.25 = 6.25\%$$

- For 2 links we 6.25% of success probability per attempt, expected 16 attempts
- For 10 links we have 0.0000001% of success probability per attempt, expected 1000000 attempts.

- For 2 links we have at most 5 attempts
- For 10 links we have at most 40 attempts.

$$\frac{10^6}{40} = 25000$$ times better for 10 links with Quantum Memory

Quantum Memories

Quantum Memories

Quantum memories are devices that store quantum states of light or matter and retrieve them later without losing their quantum properties such as superposition and entanglement.

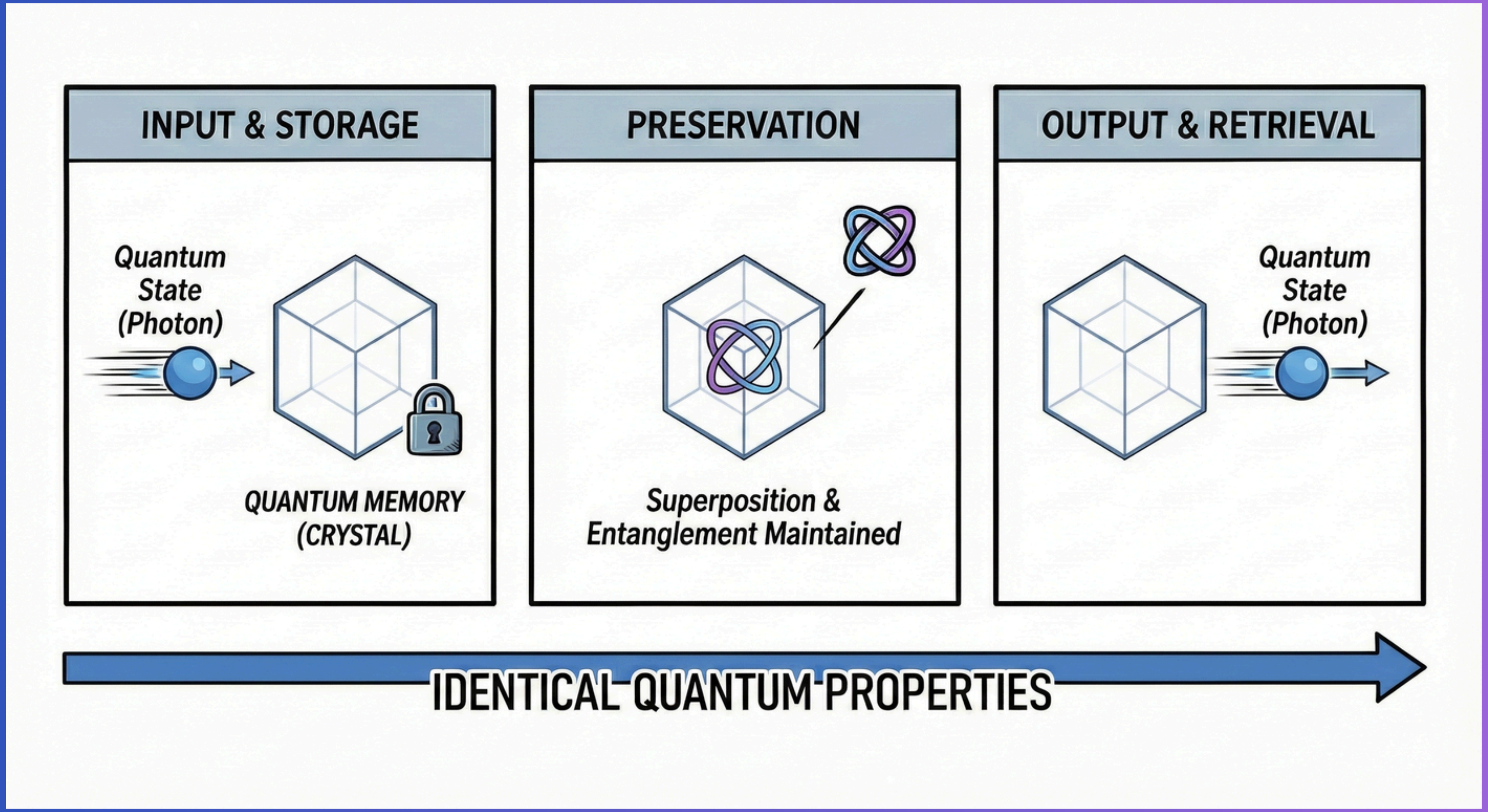

Fig 9: Basic Idea of Quantum Memories
(Image Credit: Gemini AI)

Why is Quantum Memory Hard?

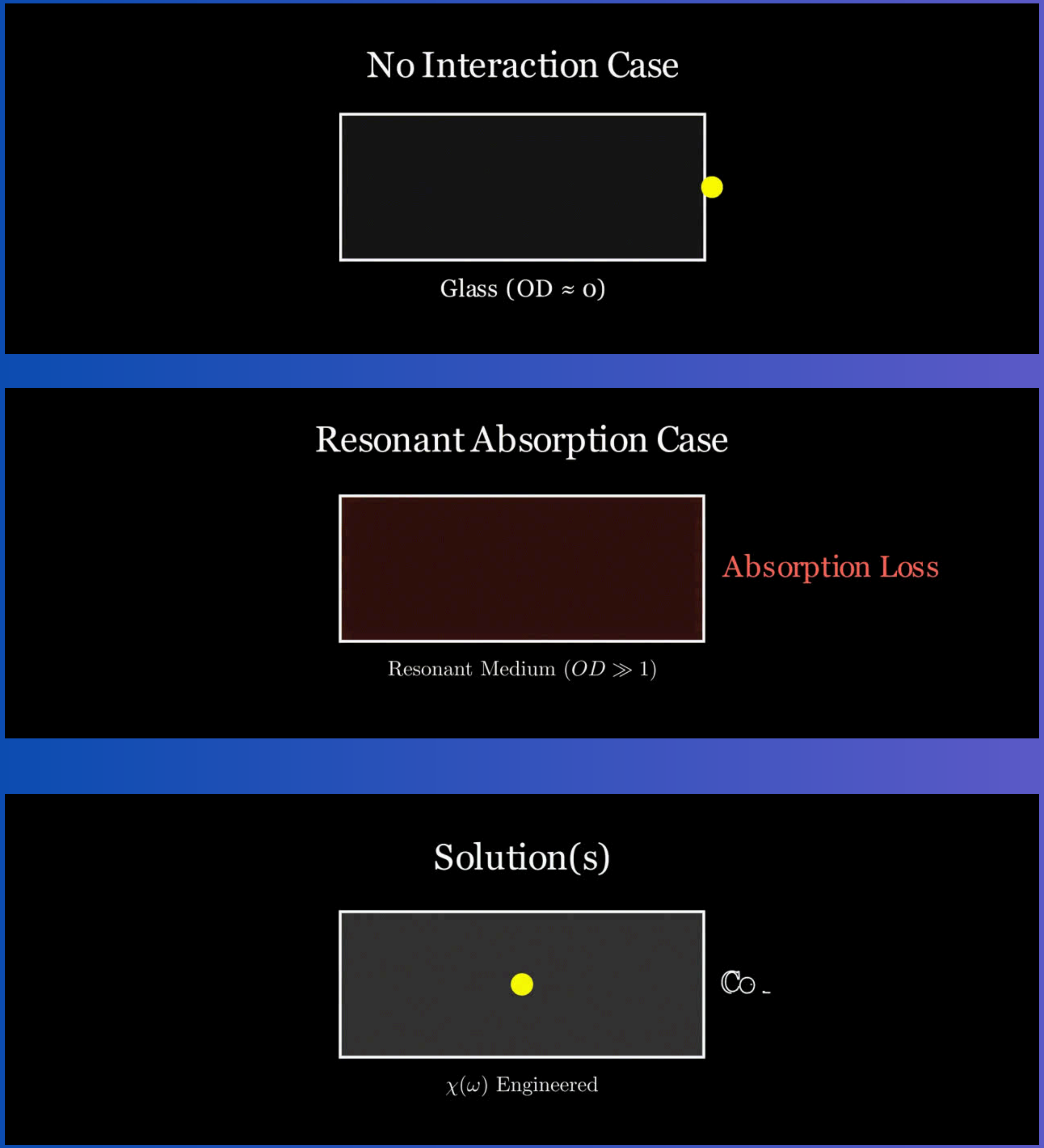

Fig 10

No Interaction of Photon with the Material

Absorption through the Medium

Solutions

Electromagnetically Induced Transparency (EIT) protocol

A technique of eleminating the effect of an absorbing medium on a propagating beam of electromagnetic radiation.

System: ^{87}Rb hot vapor (60-80°C)

$|1\rangle$ = $5S_1/_2$, F=1 (ground state 1)
$|2\rangle$ = $5S_1/_2$, F=2 (ground state 2)
$|3\rangle$ = $5P_3/_2$ (excited state)

Hyperfine splitting: Δ_HF = 6.8 GHz
Probe/Control: $\lambda \approx$ 780 nm (D2 line)

Fig 11: Destructive interference creates a transparency window within the absorption profile, altering the dispersion for Dilute Gas Atomic System like Rb-Vapours

EIT → Quantum Memory

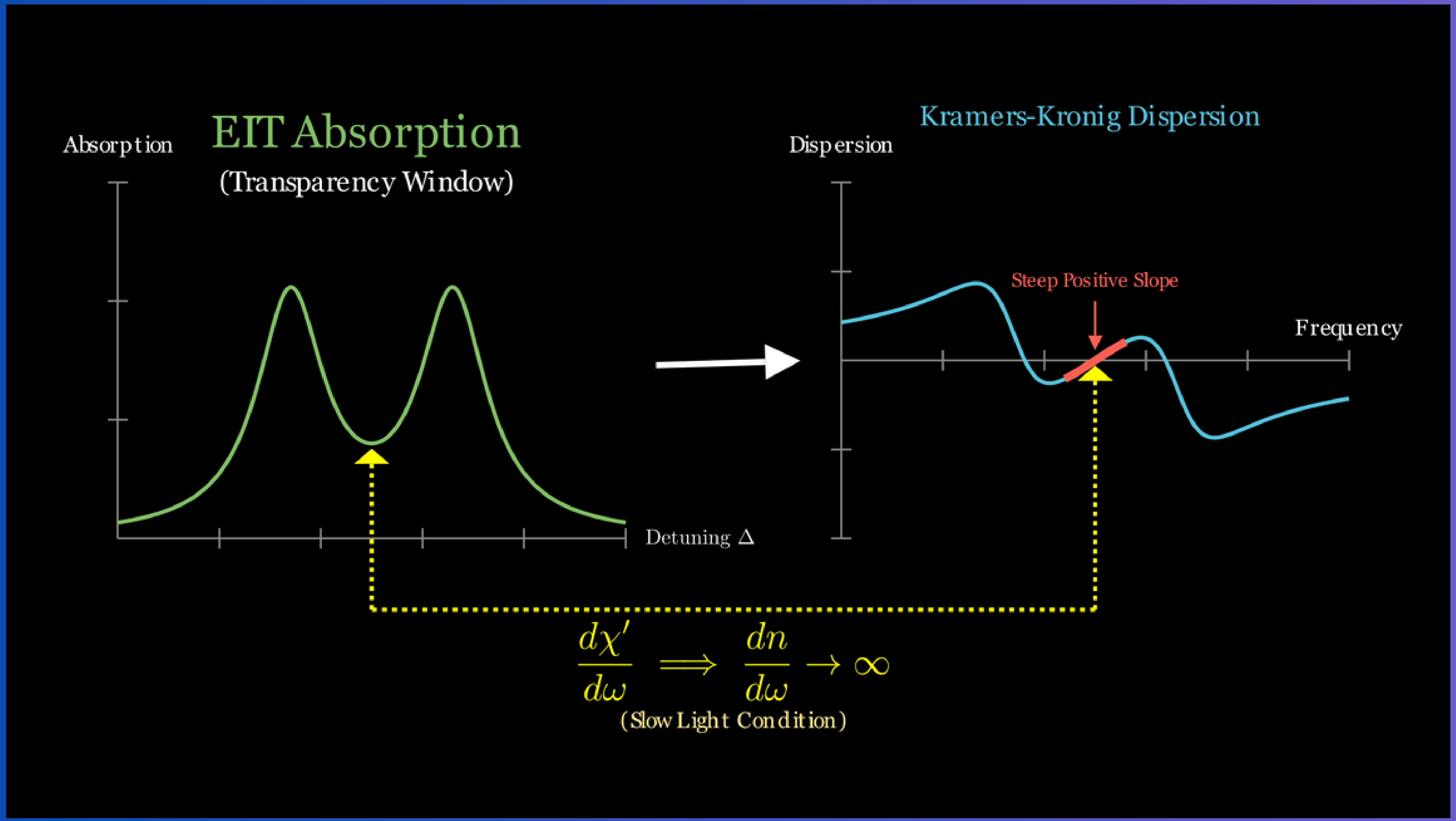

Fig 12: The steep refractive index slope results in ultra-slow group velocity

Group Velocity is given by,

$$v_g = \frac{c}{n(\omega) + \omega \frac{dn}{d\omega}} \quad (6)$$

So above eq for EIT Case becomes,

$$\text{Since } \frac{dn}{d\omega} \to \infty \implies v_g \ll c$$

The EIT transparency linewidth is proportional to the control laser intensity which is inversely proportional to rate of change of Refractive Index of the medium wrt to Frequency [1],

$$\frac{dn}{d\omega} \propto \frac{1}{\Delta\omega_{\text{trans}}} \propto \frac{1}{|\Omega_c|^2}$$

EIT → Quantum Memory (Continued)

Hence Group Velocity Eq becomes,

$$v_g \approx \frac{c}{\omega \frac{dn}{d\omega}} \propto |\Omega_c|^2 \tag{07}$$

The group velocity hits the limit bringing the pulse to a complete halt.

This shows that we can tune the Group Velocity of the light pulse that we intend to store as a memory in the medium.

So how does this connect to Memory??

EIT → Quantum Memory (Continued)

$$|\psi\rangle = \cos\theta|1\rangle - \sin\theta|2\rangle \tag{08}$$

where,

$$\cos\theta(t) = \frac{\Omega_c(t)}{\sqrt{\Omega_c(t)^2 + g^2 N}} \longrightarrow \text{The Probe Photon Component}$$

$$\sin\theta(t) = \frac{g\sqrt{N}}{\sqrt{\Omega_c(t)^2 + g^2 N}} \longrightarrow \text{Atomic Spin Wave Component}$$

$$\tan\theta(t) = \frac{g\sqrt{N}}{\Omega_c(t)} = \frac{\text{Atomic Pulling Power}}{\text{Control Opening Power}}$$

As the denominator of the tangent eq goes to zero $[\theta \to \pi/2]$
This would make cosine component 0 and Sine Component 1 $\longrightarrow$ Storage
Retrieval of this stored Information is basically the reversing this process.

That is how Quantum Memory is achieved using EIT

Atomic Frequency Comb (AFC)

Two Level System: Echo Scheme [3]

1. Preparation
   - Spectral Hole Burning (Lasers) to carve a periodic structure into the absorption profile.
   - Single photon is absorbed by the entire comb simultaneously, creating a collective "Dicke State" (superposition).
2. Dephasing and Rephasing
   - The phases evolve at different rates for different detuning frequency. Hence, the collective dipole moment vanishes rapidly. $\delta_j = n \cdot \Delta$
   - The frequencies are integer multiples of Δ, the phase factors align back

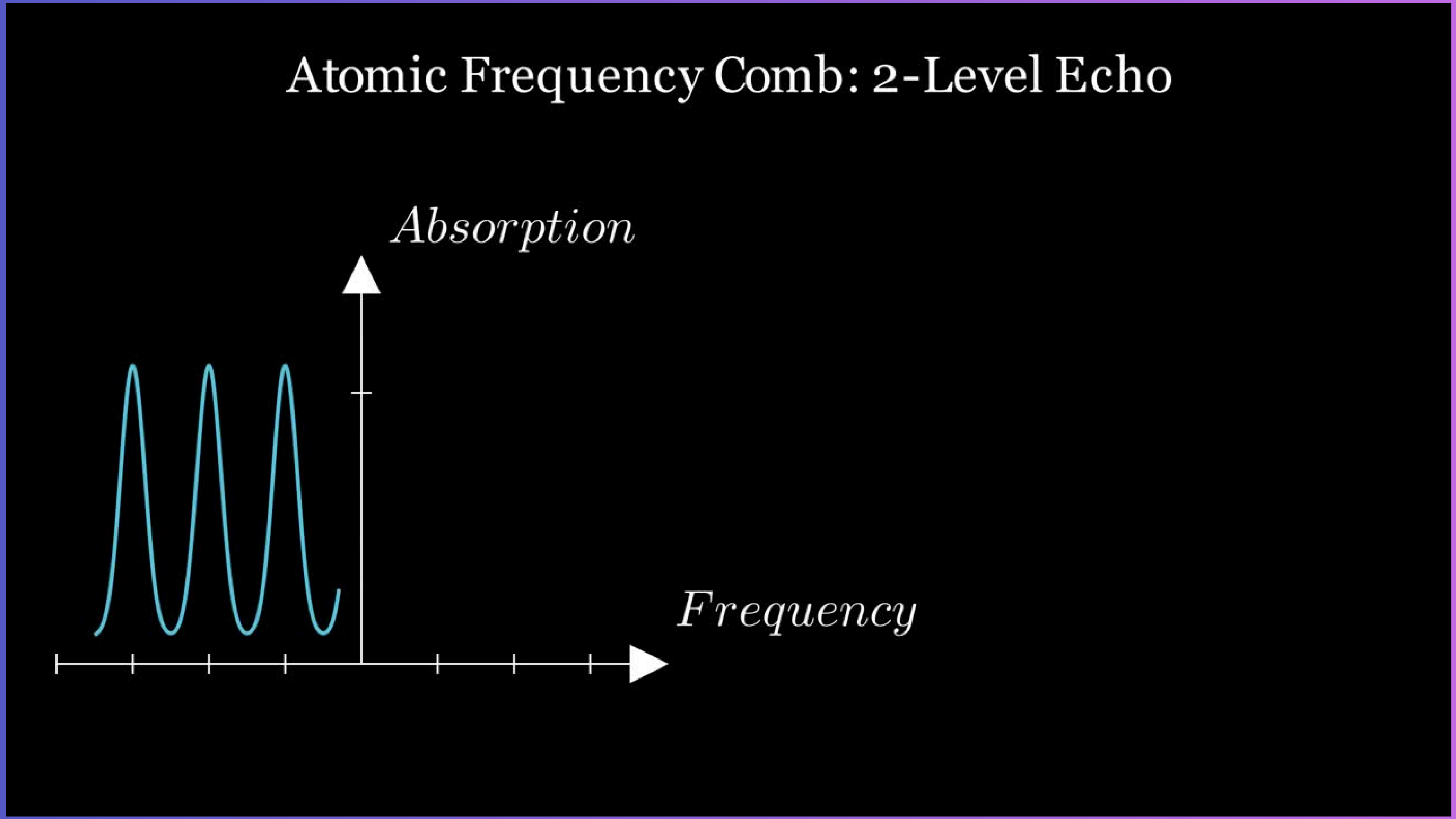

Fig 13: Periodic absorption structure acts as a diffractive element in time, creating a "photon echo" at t

$$\text{At, } e^{-i(n\Delta)t} = 1 \quad \text{when} \quad t = \frac{2\pi}{\Delta} \longrightarrow$$

The atoms constructively interfere, emitting a "Photon Echo."

AFC Continued

Three Level System: *On Demand* Emission. [3]

To achieve on-demand emission, we *transfer the excitation to a long-lived spin state, effectively 'freezing' the phase evolution* clock until retrieval.

Storage Phase

- Photon is absorbed and we know that rephasing occurs at $t = \dfrac{2\pi}{\Delta} \longrightarrow$ Echo / Emission of Photon

- *Before the Echo can occur,* we hit the system with a strong control laser $(\pi - pulse)$
- This forces the atomic state to enter Spin State from Excited State.

$$|\Psi(t_1)\rangle = \sum_j c_j e^{-i\delta_j t_1} |e_j\rangle \qquad (09) \longrightarrow \text{State before Storage (Dicke State)}$$

$$|\Psi_{spin}\rangle = \sum_j c_j e^{-i\delta_j t_1} |s_j\rangle \qquad (10) \longrightarrow \text{State during Storage}$$

AFC Continued

The Time evolution operator is simply,

$$U(T_s) = e^{-i\omega_s T_s}$$

For Storage Time T_s

This adds a global phase ϕ_s that is identical to all atoms,

$$|\Psi(t_1 + T_s)\rangle = \underbrace{e^{-i\phi_s}}_{\text{Global Phase}} \sum_j c_j \underbrace{e^{-i\delta_j t_1}}_{\text{FROZEN}} |s_j\rangle \tag{11}$$

Retrieval Phase

- After Storage time, a second control pulse maps the state back to excited state.
- Integrating the relative phase evolution. The storage interval basically contributes nothing to the relative phase.

AFC Continued

The state evolves under Excited Hamiltonian again. The total wavefunction becomes,

$$|\Psi_{final}\rangle = e^{-i\phi_{global}} \sum_j c_j \underbrace{e^{-i\delta_j(t_1+t')}}_{\text{Total Relative Phase}} |e_j\rangle \qquad (12)$$

Rephasing Condition

- Constructive interference occurs when the total relative phase equals 2π
- The physical time of emission is the sum of the active time plus the storage duration.

$$t_{emission} = \underbrace{\frac{2\pi}{\Delta}}_{\text{Echo Time}} + \underbrace{T_s}_{\text{Delay}} \qquad (13)$$

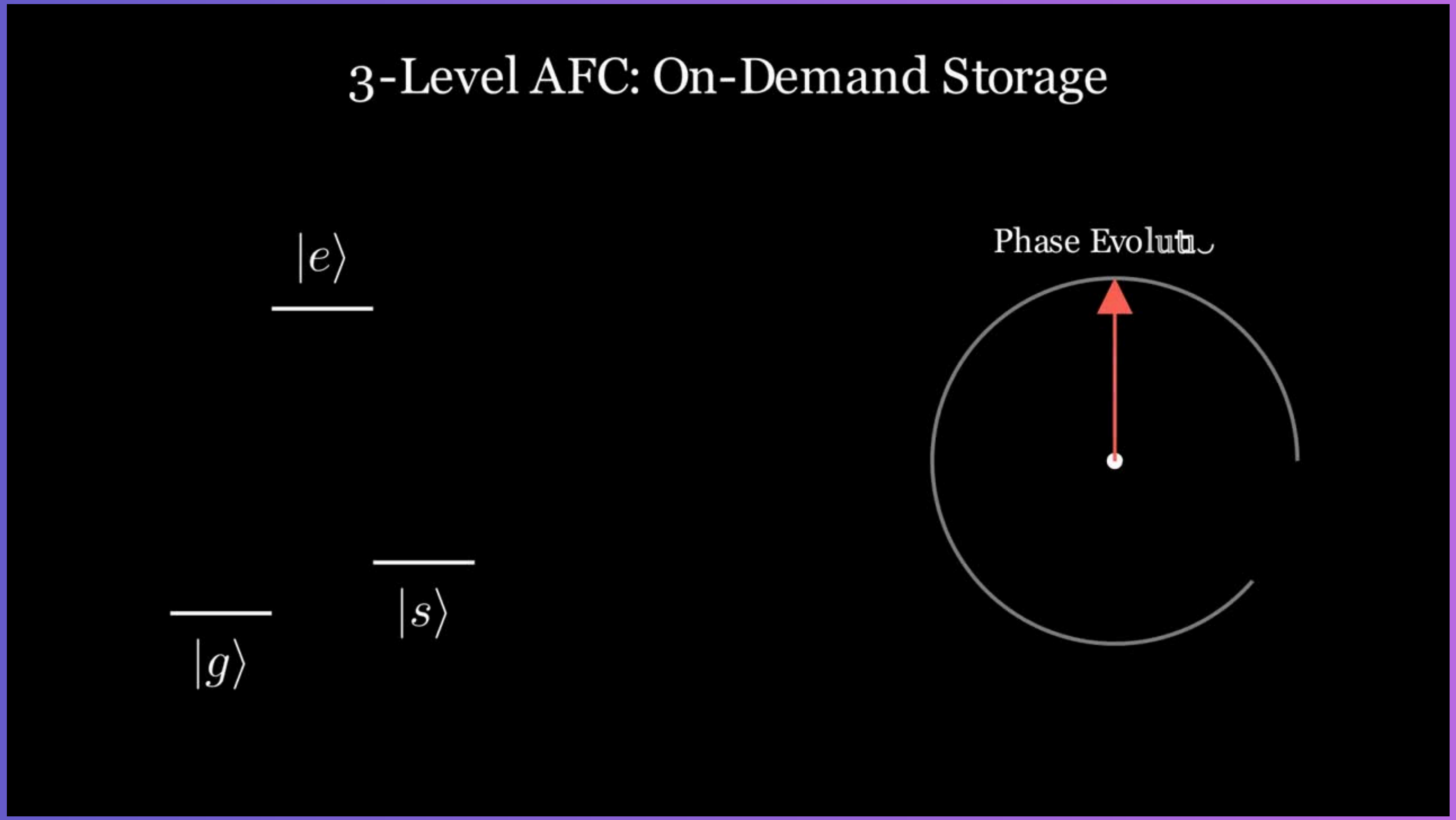

Fig 14: Application of a control pi-pulse locks the phase evolution, storing the state in the spin level until retrieval is triggered.

Types of Quantum Memories

Types of Quantum Memories

Cold Atomic Ensembles

- A cloud of neutral atoms (typically Rubidium or Cesium) cooled to near absolute zero using lasers and Magnetic field (Magneto Optical Trap - MOT)
- Excellent coherence times (ms scale) because the atoms basically aren't moving[5].
- You can get very high retrieval efficiencies up to 85(3)%[6].
- Complex and bulky setups hence hard to scale to real world network.

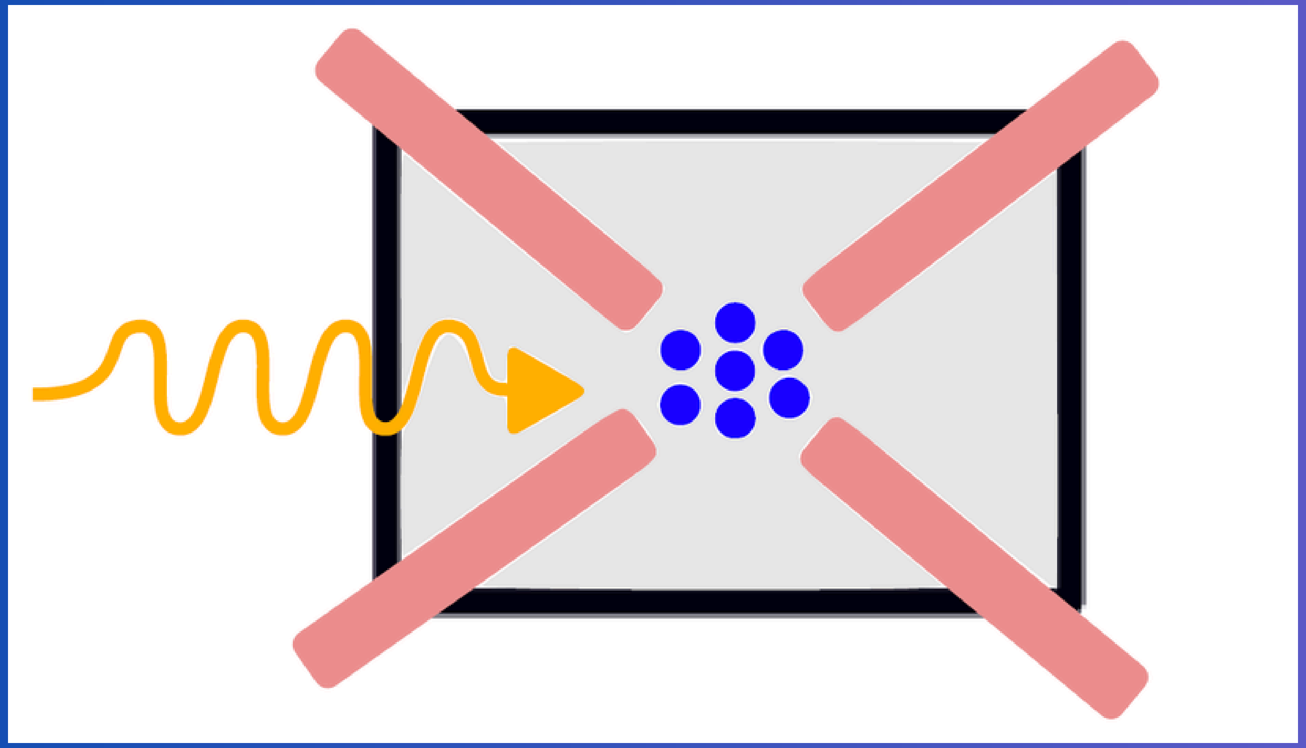

Fig 15: Illustration of Cold atomic gases in MOT,
Image Credit: Jan-Michael Mol et al 2023 Quantum Sci. Technol. 8 024006

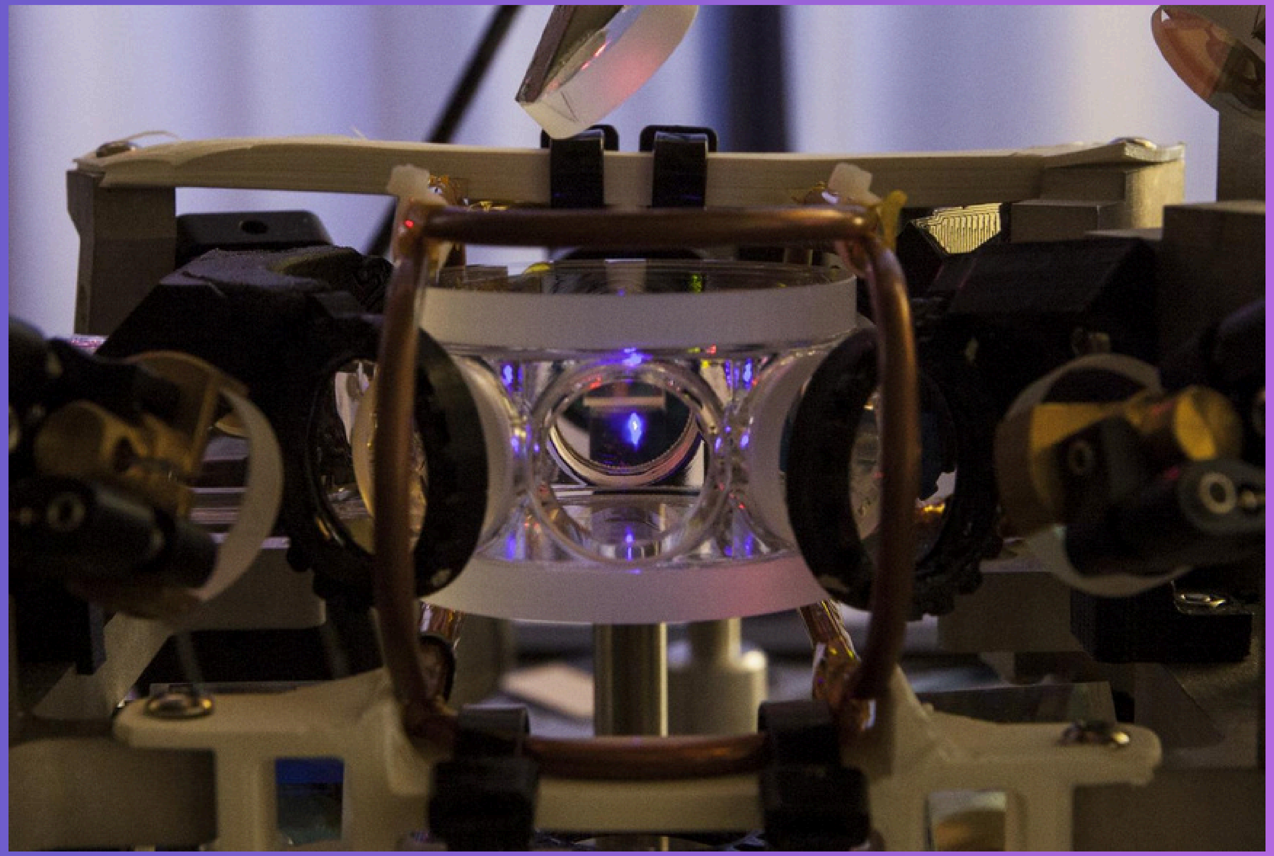

Fig 16: Cooled and trapped cloud of cold atoms used to realize the quantum memory protocol. The atoms reside in the center of the vacuum chamber, around which the magnetic coils necessary to trap the atoms are visible. The blue color is caused by two near-infrared lasers illuminating the atoms and driving a two-photon transition, which results in spontaneous emission of visible blue light. (Source: FUW, Mateusz Mazelanik)

Hot Vapour

- Glass cells containing alkali metal vapour (Rb, Cs) at room temperature (300 K) or slightly heated, eliminating the need for cryogenics.
- Demonstrated high efficiencies (up to 87%) using EIT. [8]
- High thermal motion causes Doppler broadening and collisional noise, leading to higher decoherence rates.
- Storage times are typically shorter than cold atoms due to diffusive motion of atoms out of the beam.

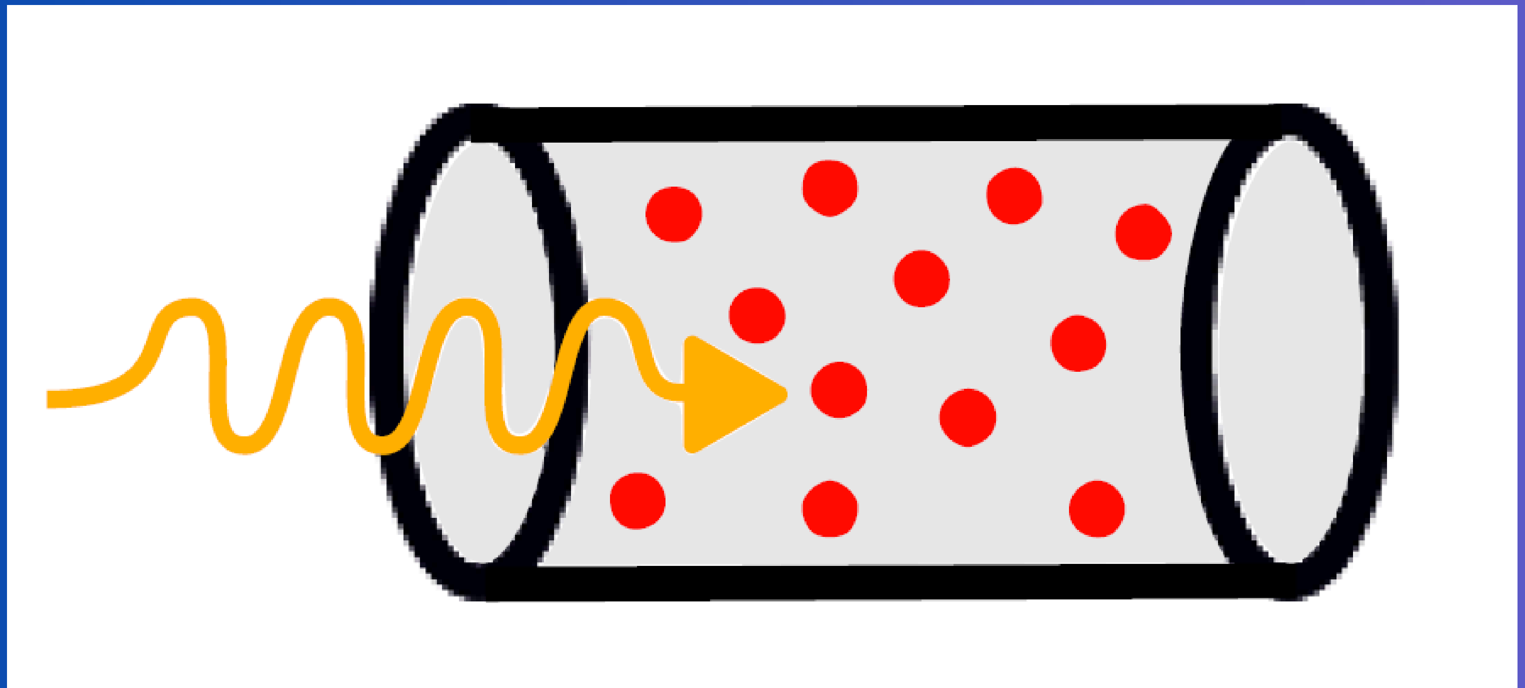

Fig 17: Illustration of Hot Vapour Cells,

Image Credit: Jan-Michael Mol et al 2023 Quantum Sci. Technol. 8 024006

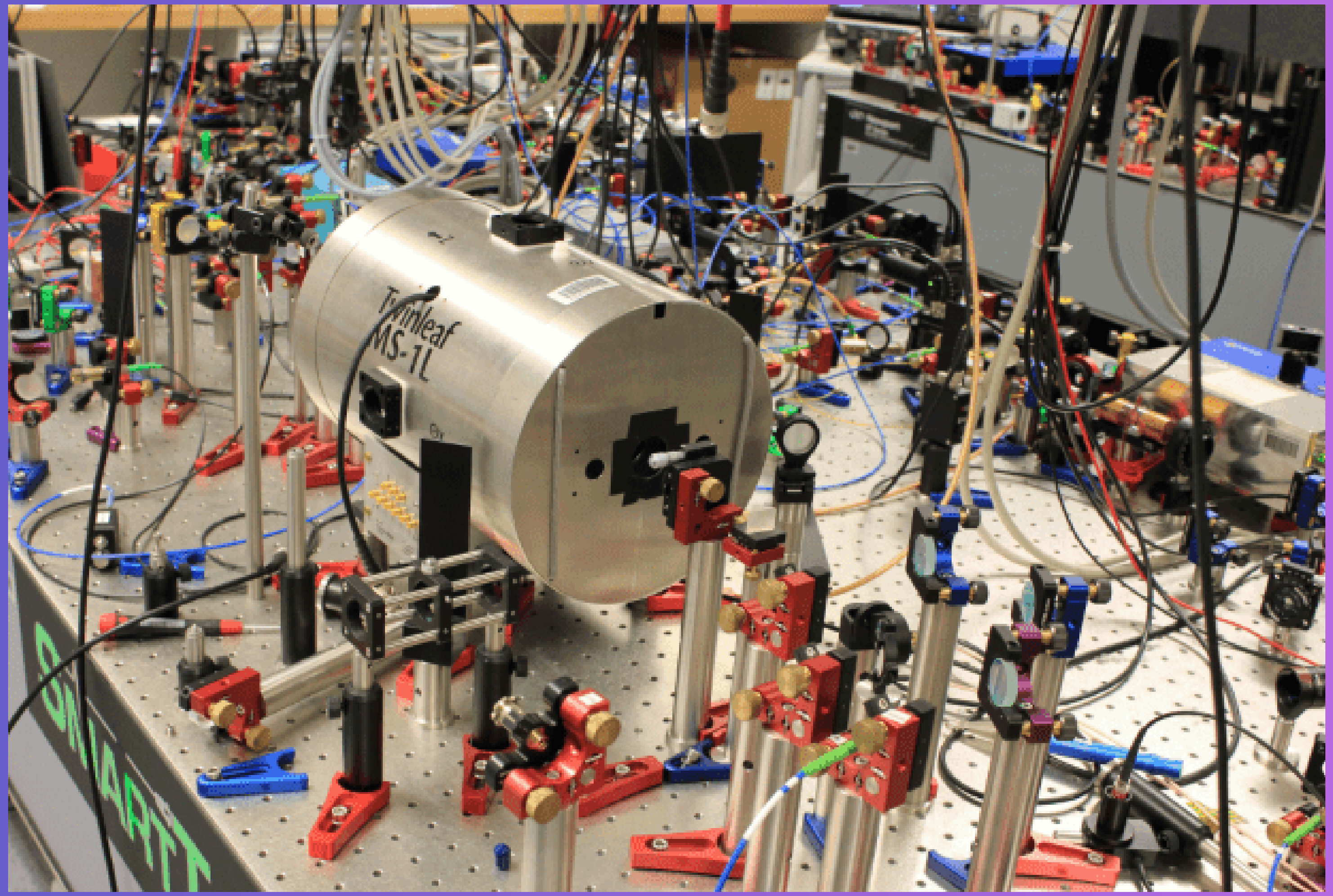

Fig 18: The University of Basel lab where the rubidium vapour cell quantum memory was developed. The vapour cell is at the centre, protected by magnetic shielding. (Courtesy: Gianni Buser)

Rare Earth Ion Doped Crystals

- Rare-earth ions (Pr^{3+}, Eu^{3+}) doped into solids (Y_2SiO_5) at cryogenic temps (<4K).
- The unique "frequency comb" structure allows storage of over 1,000 temporal modes, a key requirement for efficient quantum repeaters. [9]
- High efficiency (69%) achieved using "spin-wave storage". [10]
- Solid-state nature allows for potential integration into waveguides and fiber-coupled devices[15].
- It is mainly limited by the wavelength of the dopants.

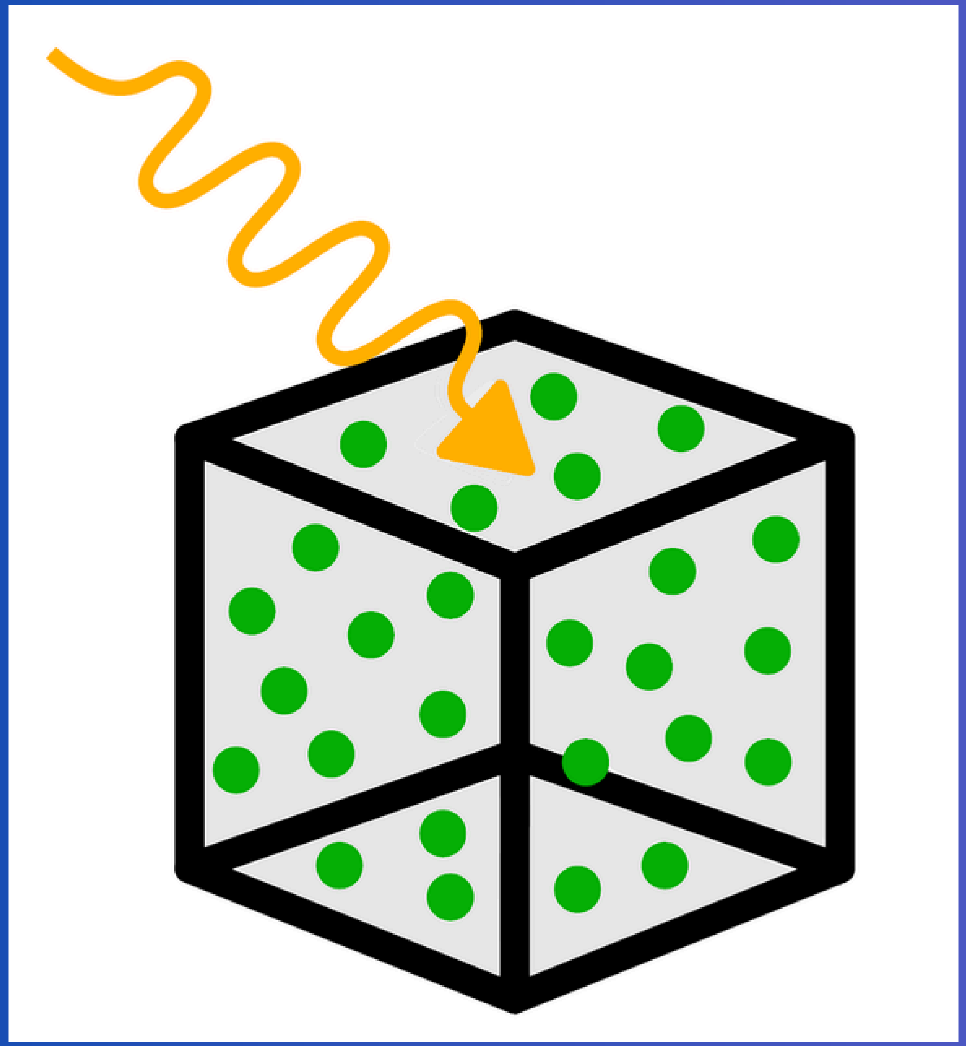

Fig 19: Illustration of Rare Earth Ion Doped Crystals,

Image Credit: Jan-Michael Mol et al 2023 Quantum Sci. Technol. 8 024006

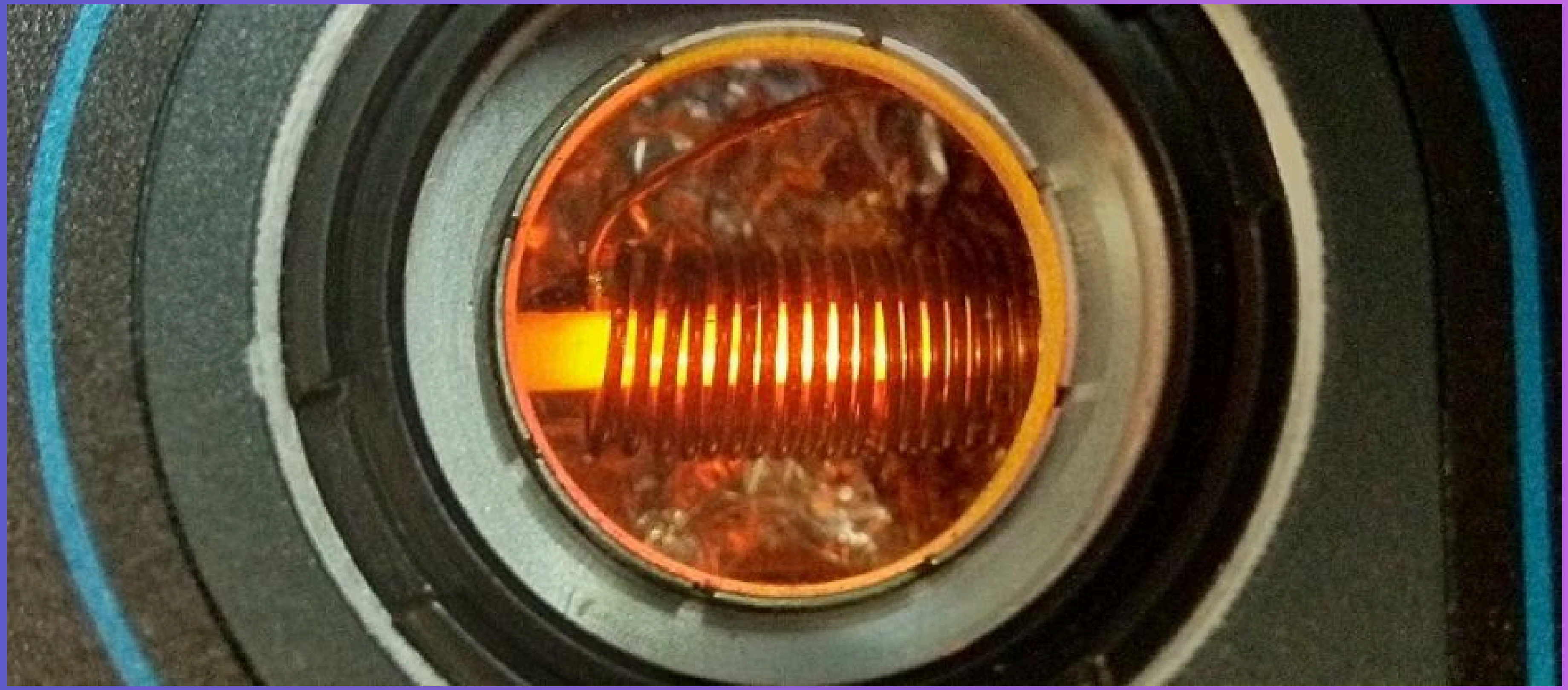

Fig 20: Crystal used for storing photonic qubits and illuminated by a laser in a cryostat, an instrument for obtaining cryogenic temperatures. (c) Antonio Ortu/CC-BY

NV Center

- A point defect in a diamond lattice consisting of a Nitrogen atom adjacent to a Carbon vacancy. It behaves like an "atom trapped in a solid".
- Can maintain quantum coherence (spin states) for milliseconds even at room temperature [11]. At cryogenics, even up to minutes (~63 seconds [12])
- Low coupling efficiency of a single photon into and out of the tiny diamond defect. Creating Identical Defect centers is an Engineering challenge

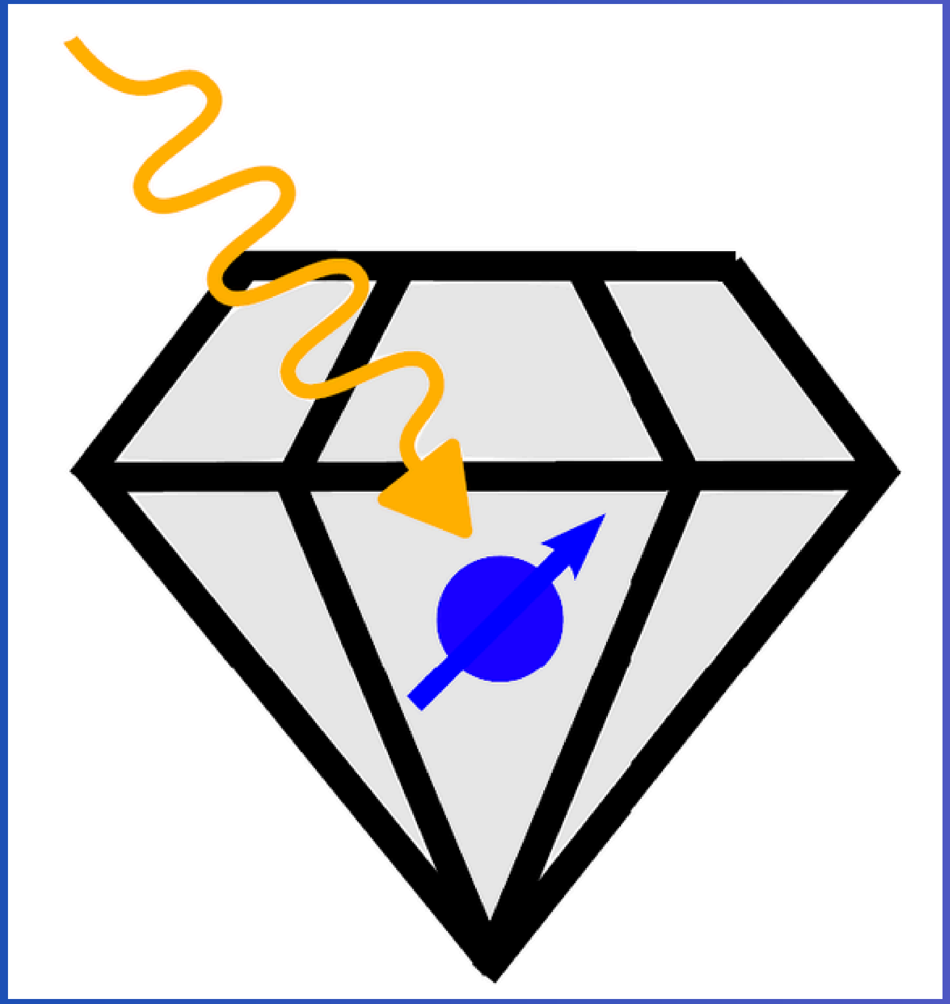

Fig 21: Illustration of NV Centers,
Image Credit: Jan-Michael Mol et al 2023 Quantum Sci. Technol. 8 024006

Fig 22: Comic Illustration of NV Centers,
Image Credit: Gemini AI

Current Implications of Quantum Memories and Repeaters

The Metropolitan Link (Delft–The Hague) [13]

Memory Type:

- Nitrogen-Vacancy (NV) Centers in Diamond.

Network Setup:

- Distance: 25 km deployed optical fiber connecting Delft and The Hague (Netherlands).
- Architecture: A "Midpoint Heralding Station" located in between the cities. Both nodes send photons to the middle to be swapped (entanglement swapping).

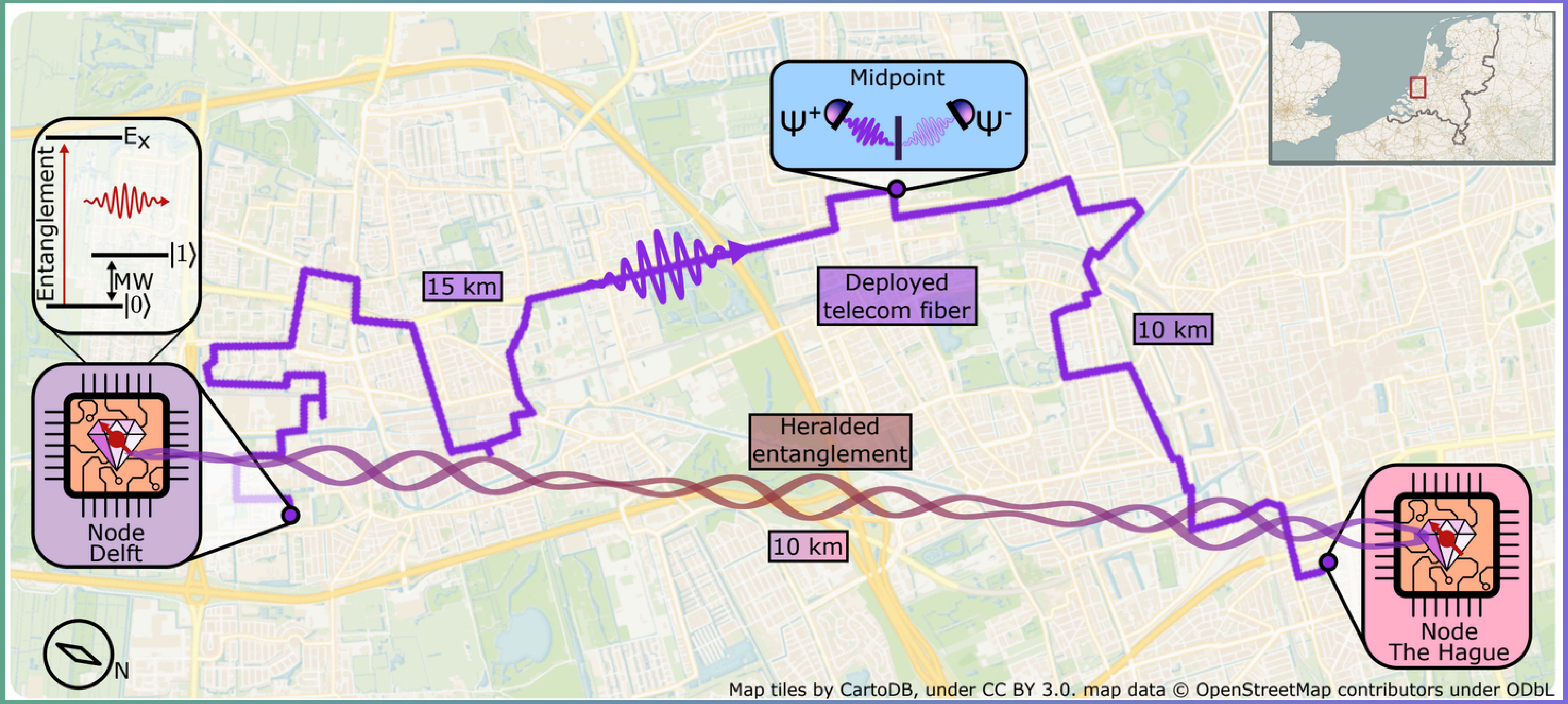

Fig 23: A metropolitan-scale quantum link connecting Delft and The Hague via 25 km of deployed commercial fiber, utilizing a central heralding station to entangle remote NV-center memories. *Image Credit: [13]*

The Metropolitan Link (Delft–The Hague)

- The NV centers emit red light (637 nm), which dies in long fibers. They used QFC (Quantum Frequency Converter) to convert this to the Telecom L-band (1588 nm) to survive the 25 km trip.

Results

- Entanglement Fidelity: ~0.80 (estimated).
    - They successfully beat the classical limit, proving entanglement exists.

Robust Entanglement via Time-Bin Qubits [14]

Memory Type: Trapped Barium Ions ($^{138}\mathrm{Ba}^{+}$).

Key Highlight: Time Bin Encoding

Results

- Entanglement Fidelity F = 97%
- Swaps "Fiber Noise" for "Atomic Motion Noise."
  - *Unresolved Trade-off: Residual Recoil effects despite Lamb-Dicke Confinement*.
- High Success probability per attempt compare to other cases.

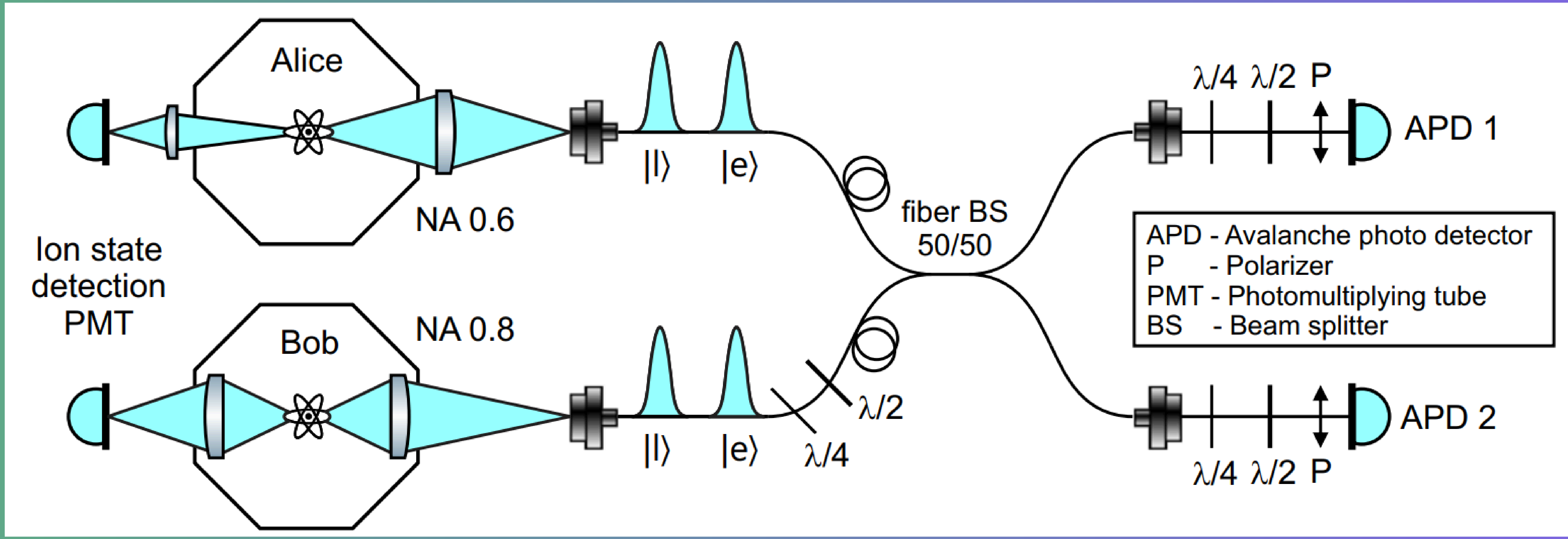

Fig 24: Two remote Barium ions entangled via time-bin photons. By encoding information in pulse timing rather than polarization, the link becomes insensitive to fiber fluctuations.

Image Credit: [14]

Future Prospects

From Optical Tables to Foundry Chips [15]

Most memories (Diamond, Rubidium) need complex frequency converters to talk to fiber.

Solution: **Erbium-doped Silicon Chips**

- First demonstration of Erbium-doped memory integrated directly onto silicon chips using standard CMOS Foundry Processes (BEOL).
- Operates natively at 1535 nm (Telecom C-Band) and connects directly to fiber with Zero Frequency Conversion required.

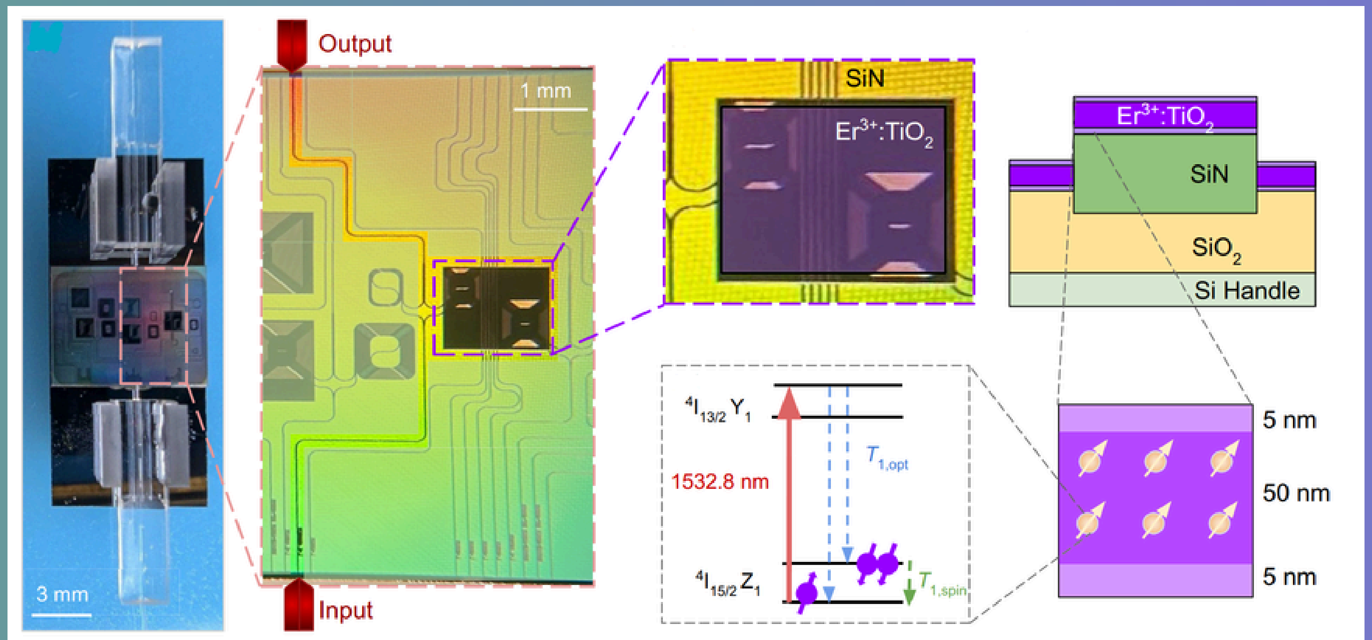

Fig 25: A microscope image and cross-section of the erbium-doped thin-film device. The memory layer $(\mathrm{Er}^{3+} : \mathrm{TiO}_2)$ is integrated directly onto standard silicon nitride (SiN) waveguides, enabling telecom-band storage on a scalable chip.
Image Credit: [15]

Results

- Optical Coherence Time of 64 μs is achieved.
- Proves we can manufacture quantum memories using standard chip-making techniques.

Conclusion

1. The Fundamental Challenge
   - Direct transmission fails due to exponential fiber loss and the No-Cloning Theorem and other factors, which prevents classical amplification.
   - We must use **Quantum Repeaters** to distribute entanglement via swapping, rather than amplifying the signal.
   - To make Quantum Repeaters possible we need **Quantum Memories**
2. The Mechanism (Protocols)
   - EIT (Electromagnetically Induced Transparency): Uses a control laser to slow light to a halt, storing it as a "dark-state polariton."
   - AFC (Atomic Frequency Comb): Uses a "comb" of absorption lines to create a photon echo, allowing for high-bandwidth multimode storage.
3. The Hardware Landscape (Trade-offs)
   - Cold Atoms: High efficiency/coherence, but requires complex laser cooling (Lab-only).
   - NV Centers & Ions: Robust and potentially scalable, but suffer from low collection efficiency or complex stabilization.
   - Rare-Earth Crystals: High bandwidth and solid-state, but require cryogenic temperatures.
4. The Current Status
   - We have transitioned from theory to Field Deployment.
   - Architecture: Commercial fiber links exist (Delft).
   - Robustness: Time-Bin encoding solves fiber noise (Ions).
   - Scalability: Foundry-based manufacturing is here (Erbium-on-Silicon).

References

1. Fleischhauer, M., Imamoglu, A., & Marangos, J. P. (2005). "Electromagnetically induced transparency: Optics in coherent media". Reviews of Modern Physics, 77(2), 633
2. Fleischhauer, M., & Lukin, M. D. (2000). "Dark-State Polaritons in Electromagnetically Induced Transparency." Physical Review Letters, 84(22), 5094–5097.
3. Afzelius, M., Simon, C., de Riedmatten, H., & Gisin, N. (2009). Multimode quantum memory based on atomic frequency combs. Physical Review A, 79(5), 052329.
4. M. Guo et al., "Rare-earth quantum memories: The experimental status quo," Frontiers of Physics, vol. 18, no. 2, Art. no. 21303, 2023.
5. Yang, S.-J., Wang, X.-J., Bao, X.-H., & Pan, J.-W. (2016). "Efficient and low-noise single-photon quantum memory." Nature Photonics, 10(6), 381–384.
6. Bao, X.-H., Reingruber, A., Dietrich, P., Rui, J., Dück, A., Strassel, T., Li, L., Liu, N.-L., & Pan, J.-W. (2012). "Efficient and long-lived quantum memory with cold atoms inside a ring cavity." Nature Physics, 8(7), 517–521.
7. Reim, K. F., Nunn, J., Lorenz, V. O., Sussman, B. J., Lee, K. C., Langford, N. K., Jaksch, D., & Walmsley, I. A. (2010). "Towards high-speed optical quantum memories." Nature Photonics, 4(4), 218–221.
8. Hosseini, M., Sparkes, B. M., Campbell, G., Lam, P. K., & Buchler, B. C. (2011). “High efficiency coherent optical memory with warm rubidium vapour.” Nature Communications, 2, 174.

9. Bonarota, M., Le Gouët, J.-L., & Chanelière, T. (2011). “Highly multimode storage in a crystal.” New Journal of Physics, 13, 013013.
10. Hedges, M. P., Longdell, J. J., Li, Y., & Sellars, M. J. (2010). “Efficient quantum memory for light.” Nature, 465, 1052–1056.
11. Maurer, P. C., Kucsko, G., Latta, C., Jiang, L., Yao, N. Y., Bennett, S. D., Pastawski, F., Hunger, D., Chisholm, N., Markham, M., Twitchen, D. J., Cirac, J. I., & Lukin, M. D. (2012). “Room-Temperature Quantum Bit Memory Exceeding One Second.” Science, 336(6086), 1283–1286.
12. Bradley, C. E., Randall, J., Abobeih, M. H., Berrevoets, R. C., Degen, M. J., Bakker, M. A., Markham, M., Twitchen, D. J., & Taminiau, T. H. (2019). “A ten-qubit solid-state spin register with quantum memory up to one minute.” Physical Review X, 9(3), 031045.
13. Stolk, A. J., et al. "Metropolitan-scale heralded entanglement of solid-state qubits." Science Advances 10, eadp6442 (2024).
14. High-fidelity remote entanglement of trapped atoms mediated by time-bin photons." Nature Communications 16, 2533 (2025)
15. Gupta, S., Pettit, R. M., Sundaresh, A., Niaouris, V., Deckoff-Jones, S., Crowley, D. P., Carpenter, L. G., Dibos, A. M., Singh, M. K., & Sullivan, S. E. (2025). Erbium Quantum Memory Platform with Long Optical Coherence via Back-End-of-Line Deposition on Foundry-Fabricated Photonics. Physical Review Applied, 24(5), 054037.
16. Sangouard, N., Simon, C., de Riedmatten, H., & Gisin, N. (2011). Quantum repeaters based on atomic ensembles and linear optics. Reviews of Modern Physics, 83(1), 33.

Appendix

- All the visualization figure 1-14 (except Fig 8) were made using Python Codes (Manim Package). This can be accessed using the following

GitHub Repo:

https://github.com/VishuVish/Quantum-Memories-and-Repeaters-Visualised

or

Just Scan the QR Code →

QnA

AFC Backup Slide

Math and Physics Behind

Hamiltonian of the Excited State

- The excited state energy explicitly depends on the comb detuning.

$$H_e|e_j\rangle = \hbar(\omega_0 + \delta_j)|e_j\rangle$$

- Phase Integral: Integrating the Energy over time t,

$$\Phi_{opt}(t) = \frac{1}{\hbar}\int_0^t \langle e_j|H_e|e_j\rangle dt' = (\omega_0 + \delta_{\mathbf{j}})t$$

- Therefore, the state evolves with detuning term active.

$$|\Psi(t)\rangle = e^{-iH_e t/\hbar}|\Psi(0)\rangle = \sum_j c_j e^{-i\omega_0 t} \underbrace{e^{-i\delta_{\mathbf{j}} t}}_{\text{Running}} |e_j\rangle$$

AFC Backup Slide

Hamiltonian of Spin State

- The spin state energy is uniform and independent of Detuning.

$$H_s|s_j\rangle = \hbar\omega_s|s_j\rangle$$

- Phase Integral: Integrating the energy over storage time.

$$\Phi_{spin}(T_s) = \frac{1}{\hbar}\int_{t_1}^{t_1+T_s}\langle s_j|H_s|s_j\rangle dt' = \omega_\mathbf{s}\mathbf{T_s}$$

The detuning term is absent in the integral.

- The state evolves only by a global phase. The relative phase from the optical domain remains fixed.

$$|\Psi(t_1+T_s)\rangle = e^{-iH_sT_s/\hbar}|\Psi_{spin}(t_1)\rangle|\Psi(t_1+T_s)\rangle = \underbrace{e^{-i\omega_sT_s}}_{\text{Global Phase}}\sum_j c_j e^{-i\omega_0 t_1}\underbrace{e^{-i\delta_j t_1}}_{\text{FROZEN}}|s_j\rangle$$